Paper No.
11269

NACE INTERNATIONAL CORROSION 2018 Conference & Expo

Localized Corrosion in the Presence of Corrosion Inhibitors at High Flow Velocities in CO_2 Environments

F. Farelas, M. Singer
Institute for Corrosion and Multiphase Technology
Department of Chemical and Biomolecular Engineering, Ohio University
342 West State Street, Athens, OH 45701, USA

D. Nugraha, S. Whitehurst
Quadrant Energy PTY LTD
Perth, Western Australia

B. Kinsella
Curtin University
5 De Laeter Way, Bentley, WA, 6102, Australia

ABSTRACT

High fluid velocities and associated shear stresses are typically encountered in oil and gas transportation pipelines and can lead to severe corrosion attack. One way to mitigate corrosion is by injection of corrosion inhibitors, which need to be effective in this challenging environment. The main objective of this research was to evaluate the performance of different commercial inhibitors with emphasis on the impact of high flow velocities under highly corrosive conditions. The importance of inhibitor concentration and effect of acetic acid was also investigated. Experiments were performed in a mid-scale flow loop, called thin channel flow cell, that enables the simulation of high flow velocities (high shear stress). Linear polarization resistance and weight loss measurements were performed to assess the inhibitors ability to decrease the general corrosion rate, while scanning electron microscopy was used for surface analysis. The occurrence of localized corrosion was evaluated by means of profilometry analysis. All the inhibitors tested showed excellent inhibition properties for general corrosion. However, localized corrosion as high as 100 mm/y was observed in some cases.

Key words: inhibition, CO_2 corrosion, localized corrosion, carbon steel

INTRODUCTION

CO_2 corrosion inhibition of carbon steel pipelines continues to be a challenge for the oil and gas industry. Implementation of effective corrosion mitigation strategies is a must to prevent the loss of production, extend the life of the pipeline and prevent catastrophic accidents. Injection of corrosion

inhibitors is one method widely used to internally protect carbon steel pipelines. Unfortunately, their efficacy under highly corrosive conditions can be drastically affected by high flow rates or high shear stress.[1] Temperature, suspended or dissolved solids and corrosion products on the steel surface could also affect the inhibitor efficcacy.[2] Persistency of the adsorbed inhibitor film on the steel surface is also important especially for batch treatment or when, for any reason the injection of corrosion inhibitor is temporally interrupted.[3]

Turbulent flow could cause localized corrosion in the presence of corrosion inhibitors that are electrostatically adsorbed on the steel surface, as reported by Mora-Mendoza el. al.[4] with quaternary amine inhibitors. A decrease on the inhibition efficiency has been observed as well due to turbulent flow and high shear stress which, according to Zeng et. al.[5], prevents the adsorption of inhibitor on the metal surface or damaged the already adsorbed inhibitor film. Still there is a debate on whether the shear stress typically found in pipelines can damage an inhibitor film or not. Xiong et. al.[6] showed, by means of atomic force spectroscopy, that the shear stress needed to remove inhibitor molecules is in the order of 50 to 100 MPa, values that are larger than those encountered in pipelines. Recently, Li et. Al. used a flow loop to demonstrate that not even 5000 Pa shear stress can cause the failure of adsorbed inhibitor on carbon steel.[7]

Considering the importance of flow effects on the performance of corrosion inhibitors, the objective of the present research was to evaluate the inhibition efficiency of five commercial corrosion inhibitors to mitigate corrosion of carbon steels at relatively high partial pressures of CO_2, in the presence of acetic, high flow velocities and high temperature. Emphasis is given to the analysis of the steel surface for localized corrosion. The results obtained from this research were crucial for the selection of the most suitable corrosion inhibitor for field application.

EXPERIMETAL SETUP AND PROCEDURE

System preparation and procedure

The experiments were conducted in a flow loop called Thin Channel Flow Cell (TCFC), Figure 1(a). The most important part is the test section (Figure 1(b)) designed in the form of a flow channel used to create well controlled fully developed turbulent flow where the shear stress can be accurately determined. It is essentially a high aspect ratio rectangular cross section (3 mm by 10 mm by 100 mm) duct equipped with four corrosion probe ports. The flow loop was first filled with 170 L of 3 wt.% NaCl solution + 106 g of $NaHCO_3$ and purged with CO_2 for 24 h. During the purging process the solution temperature was increased to 90ºC. After 24 h the oxygen concentration was measured using CHEMetrics reagent ampoules giving a concentration of around 40 ppb. Before placing (flushed mounted) the steel samples in the test section, 81 mL of acetic acid (500 ppm of free HAc) were added to the system. Afterwards, CO_2 was injected to increase the total pressure to 4 bar (3.3 bar CO_2 + 0.7 bar water vapor). The steel samples were pre-corroded for 30 minutes at a flow velocity of 5 m/s before adding the selected inhibitor. In a single test, the flow velocity was increased from 5 m/s to 7.5 m/s and 10 m/s, respectively, every 6 hours. After the test, two samples were used for weight loss and one for surface analysis. Experimental conditions are summarized in Table 1.

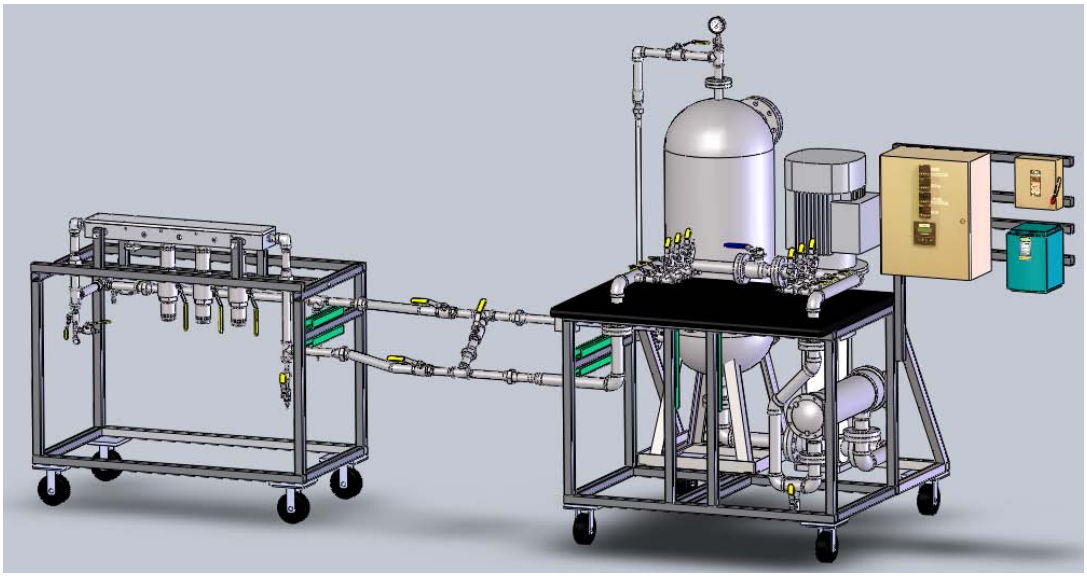

(a)

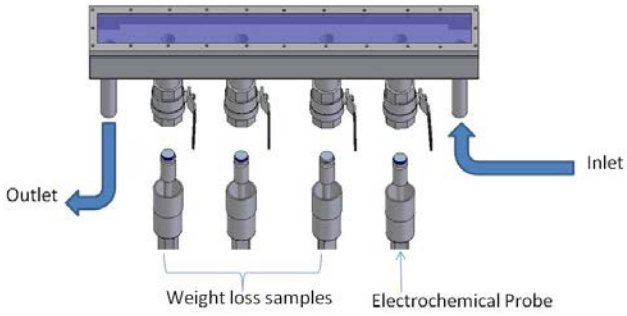

(b)

Figure 1: (a) Schematic of the TCFC system, (b) Test section.

Table 1: Experiments matrix for continuous injection tests.

Operating parameters	**Conditions**
Test solution	3 wt.% NaCl + 500 ppm Total Acetate Species
Test material	API 5L X65
Temperature (°C)	90
Total pressure (bar)	4
pCO_2 (bar)	3.3
pH	5 ± 0.01
Flow rate (m/s)	5, 7.5 and 10 m/s (60, 120 and 200 Pa shear stress)
Inhibitors	A, B, C, D, E
Corrosion rate measurements	Linear polarization resistance (LPR) and weight loss (WL)
Surface analysis	Scanning electron microscopy (SEM), energy-dispersive X-ray spectroscopy (EDS), Profilometry

Samples characteristics and preparation

Weigh loss samples (WL) and working electrode (WE) for electrochemical measurements were made of API 5L[(1)] X65 steel (chemical composition is shown in Table 2). The electrochemical probe (Figure 2(a)) consisted of a working electrode (WE) with an exposed are of 0.95 cm^2 and counter electrode

([1]) American Petroleum Institute (API), 1220 L St. NW, Washington, DC 20005.

(CE) made of stainless steel. A $Ag/AgCl_2$ electrode was used as reference. The WL samples (Figure 2(b)) were machined in a cylindrical shape of 3.17 cm diameter and 0.64 cm long. The sides and the back were coated with a fluoropolymer leaving an exposed area of 7.9 cm^2. Prior to inserting in the test section, the electrochemical probe and three weight loss samples were ground by silicon carbide paper to 600 grit and rinsed with isopropyl alcohol. The samples' weight was recorded for further weight loss corrosion rate calculation.

Table 2: Chemical Composition of API 5L X65 steel used in the TCFC tests (wt.%)

API 5L X65 mild steel (balance Fe)										
Al	**As**	**C**	**Co**	**Cr**	**Cu**	**Mn**	**Mo**	**Nb**	**Ni**	**P**
0.033	0.015	0.140	0.012	0.150	0.140	1.180	0.160	0.027	0.380	0.012
S	**Sb**	**Si**	**Sn**	**Ti**	**V**	**Zr**				
0.003	0.035	0.250	0.012	0.002	0.052	0.004				

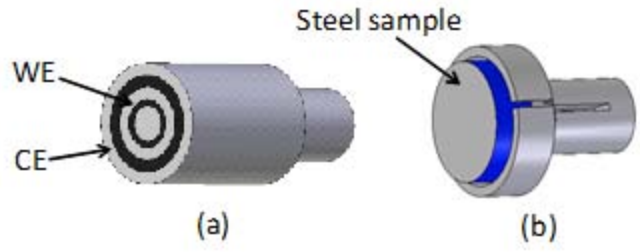

Figure 2: (a) LPR probe head, (b) cylindrical mild steel weight loss sample.

Electrochemical measurements

LPR measurements were performed using a Gamry† PCI4/300 Potentiostat/Galvanostat/ZRA. The working electrode was polarized ±10 mV versus the open circuit potential using a scan rate of 0.125 mV s^{-1}. The polarization resistance, Rp, was used to calculate the current density (j_{corr}) by using the Stern-Geary equation.[8] The resulting j_{corr} was converted into corrosion rate using Equation (1):

$$\text{Corrosion rate(mm/y)} = \frac{0.00327 \times j_{corr}(\mu A/cm^2) \times EW}{\text{density}(g/cm^3)} \quad (1)$$

where 0.00327 is a constant factor used unit conversion and EW is the equivalent weight of iron in grams.

Surface analysis

Analysis of the morphology and chemical composition of the corrosion product formed after the test was performed on a JEOL† JSM-6390LV instrument and EDAX† EDS detector, respectively. The pit depth was measured after removal of the corrosion product using a profilometer from Alicona†.

† Trade name.

Tested corrosion inhibitors

Five commercial corrosion inhibitors were tested with the aim of selecting the best inhibitor for field application. The selected chemicals contained functional groups found in corrosion inhibitors for CO_2 corrosion, e.g. thiol, amine, imidazole. The exact chemical composition of the tested corrosion inhibitors cannot be disclosed.

RESULTS AND DISCUSSION

Baseline Conditions: Effect of HAc in CO_2 corrosion in the absence of corrosion inhibitor

The presence of acetic acid (HAc) enhances the corrosion rate of carbon steels exposed to CO_2 corrosion. Tran et. al.,[9] recently showed that HAc acts as a buffer, acting as a source of hydrogen ions in addition to carbonic acid (H_2CO_3) and bicarbonate (HCO_3^-) when CO_2 is present. Figure 3 shows the results obtained without corrosion inhibitors. As mentioned earlier, the flow velocity was changed stepwise from 5 m/s to 7.5 m/s and 10 m/s in one single test. Figure 3(a) shows the change of corrosion rate with time measured with the LPR technique. It is important to mention that the B value, used to calculate the corrosion rate, was calibrated with the weight loss measurements shown in Figure 3(b). For the tests with HAc a B value of 79 mV/dec was calculated while a value of 115 mV/dec was used for the tests with no HAc. These are very high values that are not easy to justify theoretically. One possibility is that the corrosion current was close to the cathodic limiting current. However, one cannot be sure without a more detailed electrochemical investigation, as presented by Li et al.[7]

More than a twofold increase is clearly seen in the corrosion rate when HAc acid is present. Another important observation is that at the experimental conditions the corrosion rate is independent of the flow velocity, which means that the corrosion process is not under mass transfer controlled. This is to be expected as the large velocities the limiting currents. However, after a couple hours, the corrosion rate returned to the initial value observed before increasing the flow velocity. The corrosion rate measured by weight loss (WL) is shown in Figure 3(b). Similar to the LPR results, the WL loss measurements showed that with HAc the corrosion almost doubled.

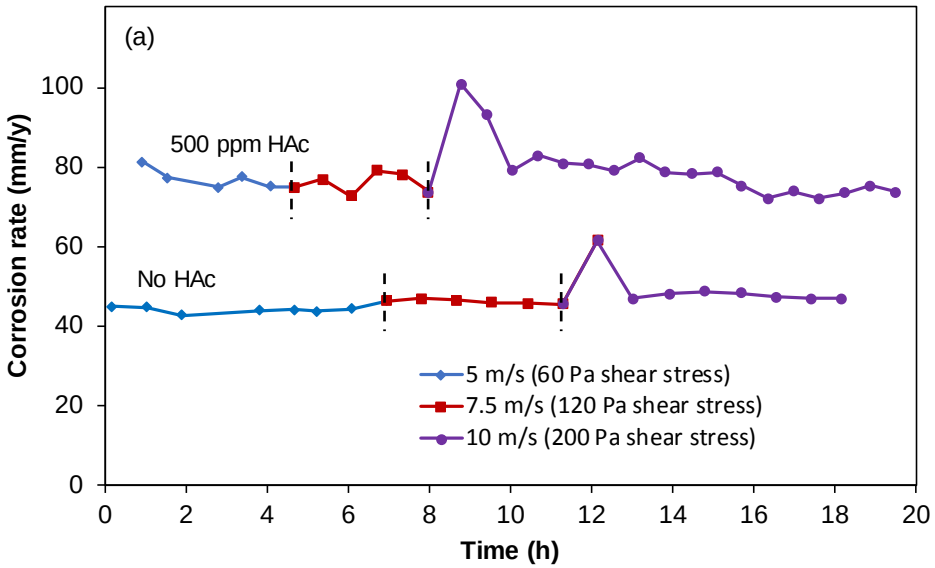

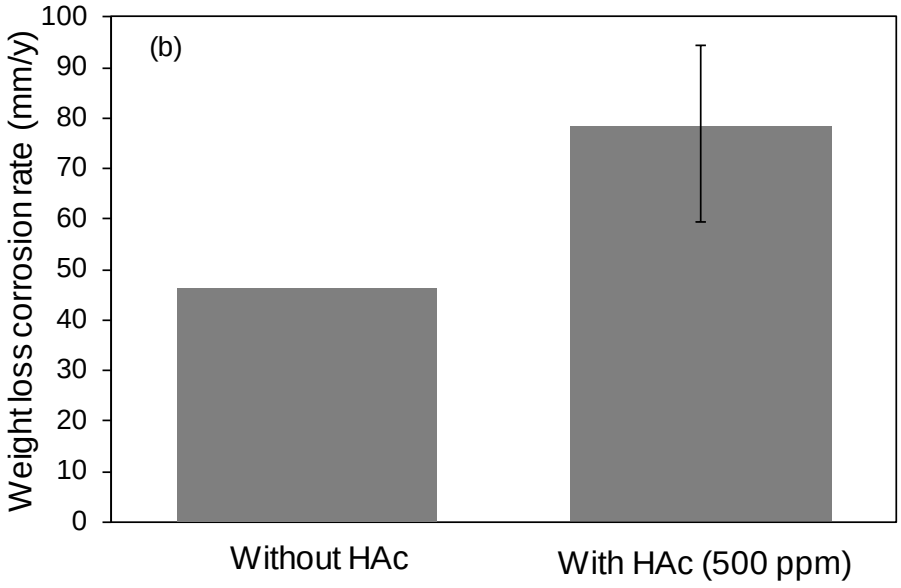

Figure 3: (a) LPR corrosion rate measured at different flow velocities, (b) Average weight loss corrosion rate. (90ºC, *p*CO2 = 3.3 bar).

Figure 4 shows the surface and cross-section SEM pictures of a steel sample exposed to CO_2 corrosion without HAc and without inhibitor. A porous layer that has been identified in other similar studies[10,11,12] as Fe_3C, is evident specially in the cross-section view. It is important to mention that localized corrosion was not observed in neither of the samples from these two baseline tests.

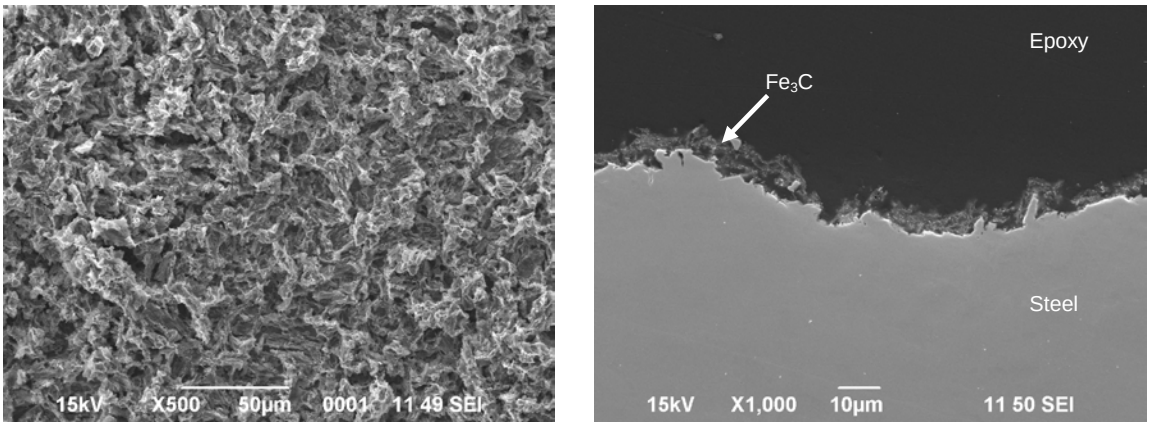

Figure 5: SEM surface and cross-section analysis of the steel samples for test with no HAc. (90ºC, *p*CO2 = 3.3 bar).

Evaluation of corrosion inhibitors

As shown in the previous section, the corrosion rate of carbon steel at different flow velocities exposed to CO_2 in the presence and absence of HAc is significantly different, but both are very high corrosion rates. Therefore, to preserve the integrity or extend the life of pipelines it is important to select a corrosion inhibitor that will withstand the harsh field conditions, high levels of CO_2, high flow velocities or shear stress and presence of organic acids. The following section shows the corrosion rates and surface analysis of carbon steel samples after the addition of five different corrosion inhibitors. As mentioned earlier the exact chemical composition of these commercial chemical packages was not disclosed.

Corrosion rate

Figure 6 shows the change in open circuit potential (OCP) and LPR corrosion rate before and after the addition of 400 ppm of a corrosion inhibitor. The selection of this inhibitor concentration was based on a preliminary test where 100 ppm of inhibitor “A” was injected. That concentration just decreased the WL corrosion rate to 24.4 mm/y. For that reason, it was decided to use 400 ppm for all the tested inhibitors. It is important to point out that the purpose of this research was to select the best inhibitors for field application and not to find the optimum concentration for all of them.

The corrosion potential shown in Figure 6(a) shifted to more positive or noble potentials after the addition of corrosion inhibitor which has been ascribed to the adsorption of inhibitor molecules on the steel surface.[13,14] Usually the corrosion potential remains at more positive values after adding corrosion inhibitors, however in these experiments the OCP shifted again to more negative potentials with time. A similar behaviour was observed by Mora-Mendoza et. al.[4] using a rotating cylinder electrode. There was a slight change in OCP after each flow velocity increase, however, there was no clear effect of flow velocity since the OCP constantly changed throughout the test.

Figure 6(b) shows the change in corrosion rate with time before and after the addition of 400 ppm of corrosion inhibitor. The corrosion rate decreased sharply for all inhibitors tested, being fastest for “C” and slowest for “D” during the first 6 h of exposure. After increasing the flow velocity from 5 m/s to 7.5 m/s and 10 m/s, respectively, the trend in the corrosion rate did not change, which suggests that, in the presence of these inhibitors (400 ppm), the corrosion rate was independent of flow rate. There was no evidence of reaching a critical flow velocity where the inhibitor film was removed from the steel surface, or even affected, as would be indicated by a sudden increase in the corrosion rate. The inhibitors efficiency (IE) is included in Figure 6(b) which is higher than 99% for all the chemicals tested.

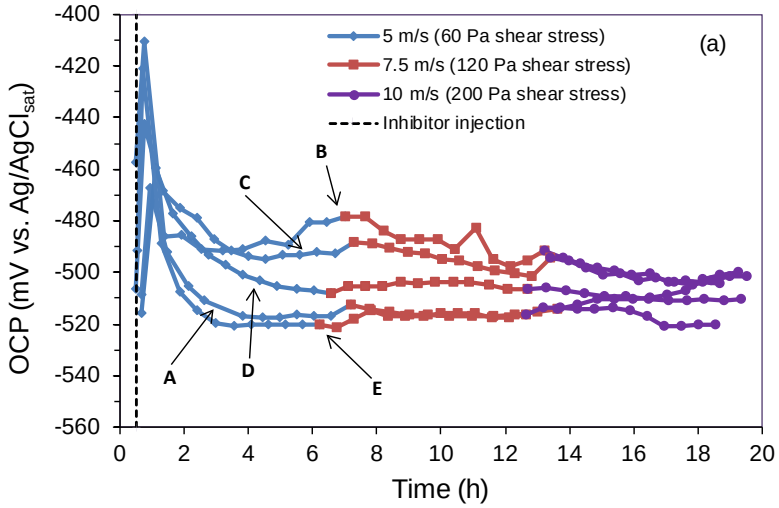

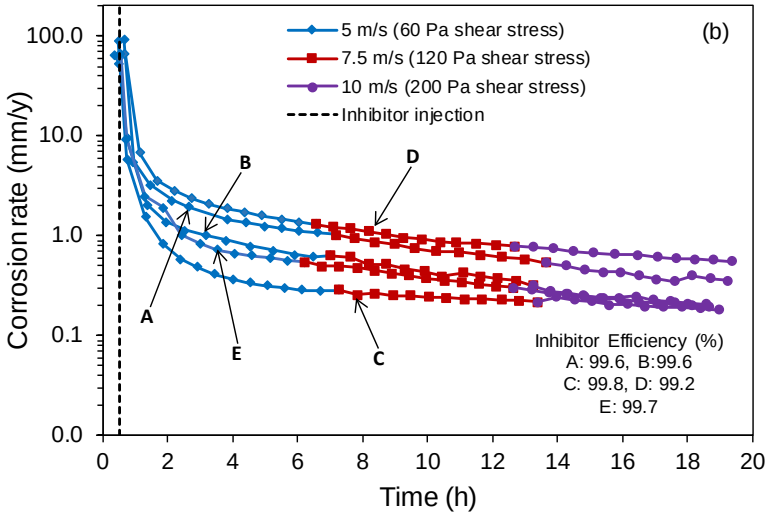

Figure 6: (a) Open circuit potential and (b) LPR corrosion rate change after injecting 400 ppm of corrosion inhibitors. (90ºC, *p*CO2 = 3.3 bar, HAc = 500 ppm).

The average weight loss corrosion rate is displayed in Figure 7. The result for the test without corrosion inhibitor was included for comparison. It is important to mention that the weight loss corrosion rates with inhibitor included the mass loss during the pre-corrosion time. It is clear that inhibitors "B" and "E" performed a little better than the rest of chemicals. However, these results are still not conclusive to select the best corrosion inhibitor for field application.

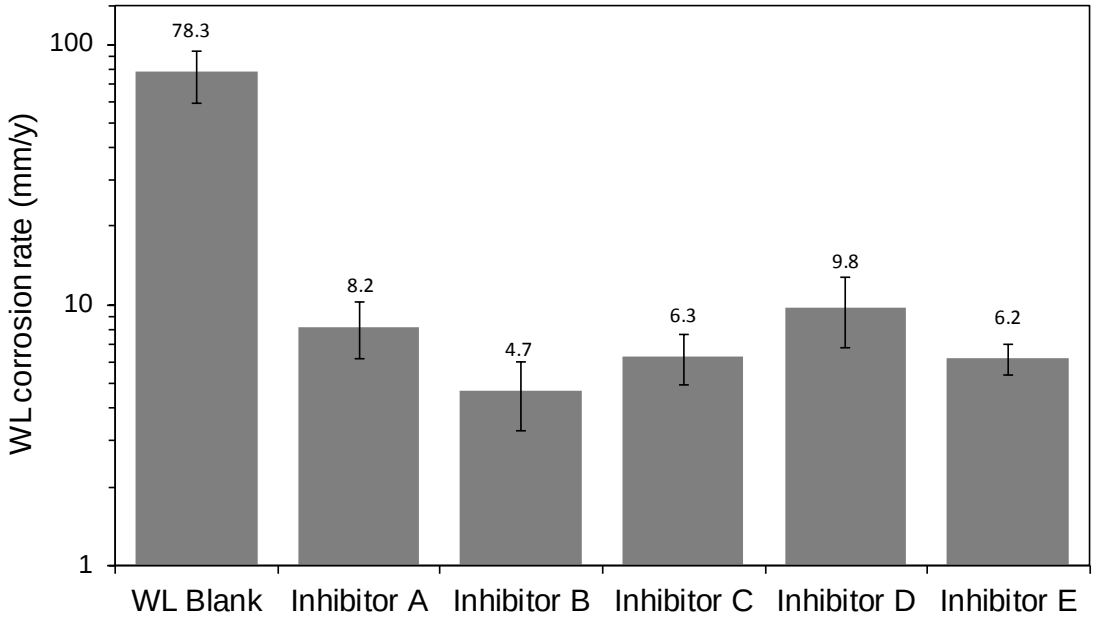

Figure 7: Comparison of the weight loss corrosion rate for the five corrosion inhibitors tested. (90ºC, *p*CO2 = 3.3 bar, HAc = 500 ppm).

Surface analysis after removal of corrosion products

Further analysis of steel surface after removal of the corrosion products was performed to look for any signs of localized corrosion. Figure 8 clearly shows localized attack for the experiments with 400 ppm of inhibitors “A”, “C” and “D”. Inhibitors “B” and “E” performed better at the experimental conditions and the 400 ppm injected seemed to be suitable to decrease the general corrosion rate (Figure 7) without the occurrence of localized attack. It is evident that the electrochemical or weight loss measurements, shown in the previous sections, could not determine the likelihood of localized corrosion. Mora-Mendoza et. al.[4] reported that changes in the OCP to more positive values after increasing the rotation speed are a sign of the removal of the electrostatically adsorbed corrosion inhibitor and the reason of the localized attack observed on their studies. However, the OCP measurements shown in Figure 6(a) did not show any trend that could give a hint about the development of localized attack in these experiments.

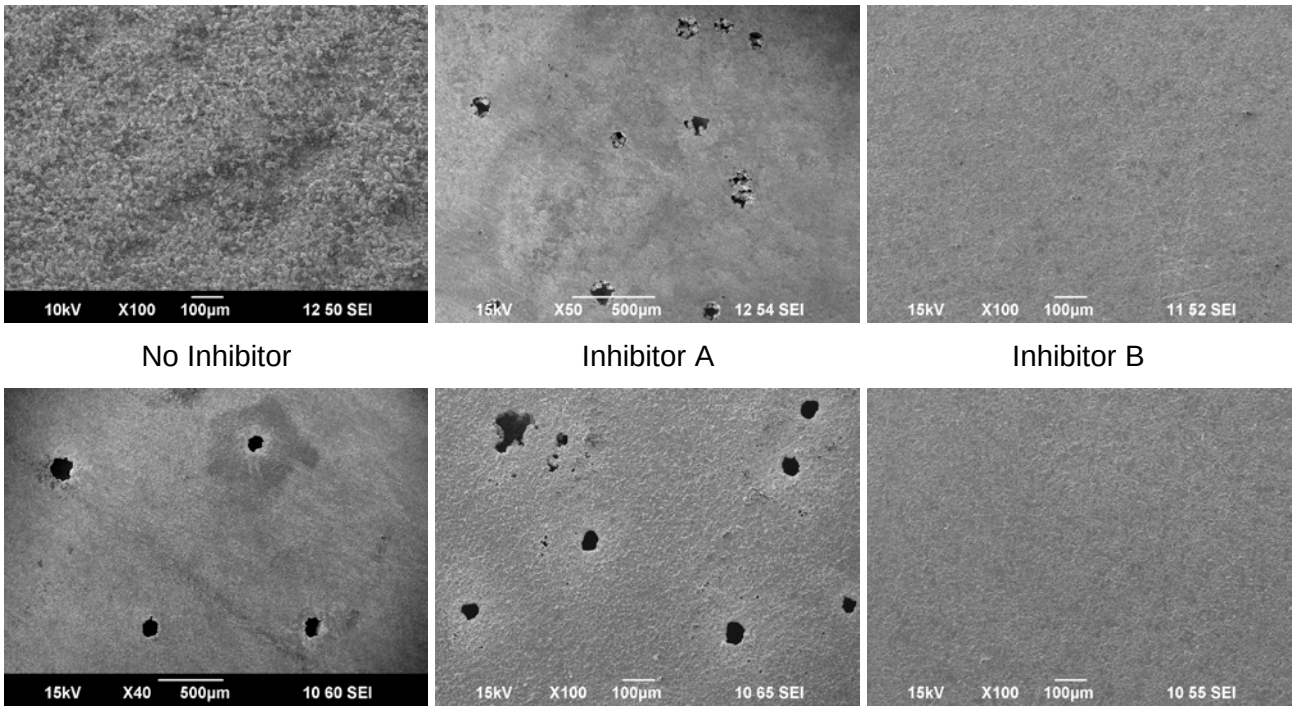

Figure 8: SEM surface analysis of the steel samples after removal of the corrosion products. (90°C, *p*CO2 = 3.3 bar, HAc = 500 ppm).

In order to measure pit’s depth and calculate the localized corrosion rate, profilometry analysis was performed on the samples for the tests with inhibitors “A”, “C” and “D”. The results are shown from Figure 9 to Figure 11. The severity of the localized attack was assessed by measuring depths of up to 229.8 μm for the case of the test with inhibitor “C” which represents a pit penetration rate of 100.6 mm/y. It is important to emphasize again that when corrosion inhibitor efficiencies are evaluated, their ability to prevent localized corrosion is important.

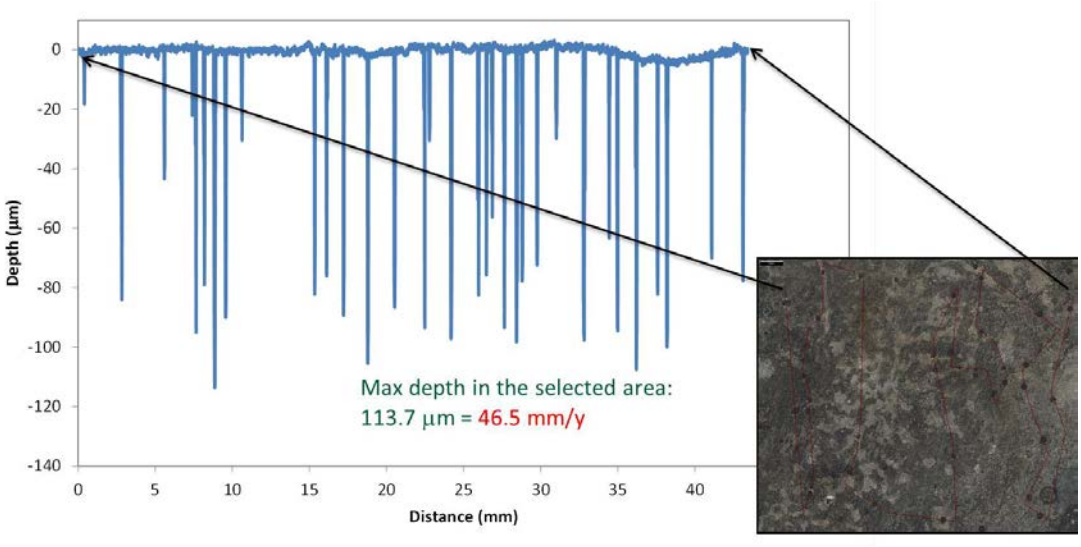

Figure 9: Surface profilometry analysis a steel sample for the test with inhibitor "A". Based on the deepest pit (113.7 µm) localized corrosion rate was 46.5 mm/y.

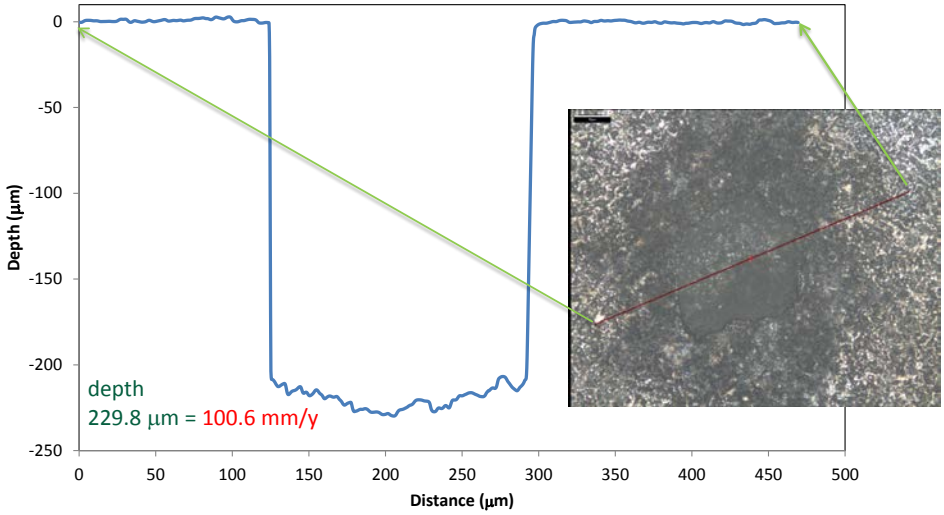

Figure 10: Surface profilometry analysis a steel sample for the test with inhibitor "C". Based on the deepest pit (229.8 µm) localized corrosion rate was 100.6 mm/y.

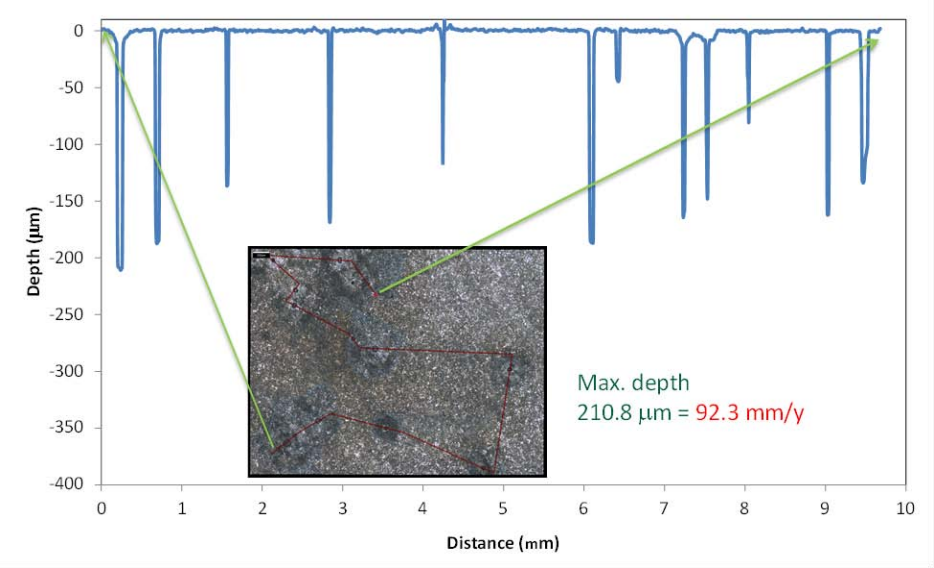

Figure 11: Surface profilometry analysis a steel sample for the test with inhibitor "D". Based on the deepest pit (210.8 µm) localized corrosion rate was 92.3 mm/y.

Effect of inhibitor concentration

In the previous section no localized corrosion was observed for inhibitors "B" and "E" at a concentration of 400 ppm. To investigate the effect of inhibitor concentration on performance, inhibitor "B" was selected for further testing as it gave the lowest general corrosion rate. Figure 12(a) compares the LPR corrosion rate change with time at concentrations of 200 ppm and 400 ppm. At both concentrations, the corrosion rate is independent of the flow velocity as no change was observed after increasing to 7.5 m/s and 10 m/s, respectively. However, the corrosion rate is time dependent. It can be noticed as well that the corrosion rate decreased faster after the addition of 400 ppm. After 4 h of exposure there is no major difference between the two concentrations. In contrast, the WL and pitting corrosion rate, depicted in Figure 12(b), showed important differences for the two concentrations. The WL corrosion rates was 8.4 mm/y for 200 ppm and 4.2 mm/y for 400 ppm. In addition, localized corrosion was observed with to 200 ppm which means that this concentration is not suitable at these experimental conditions.

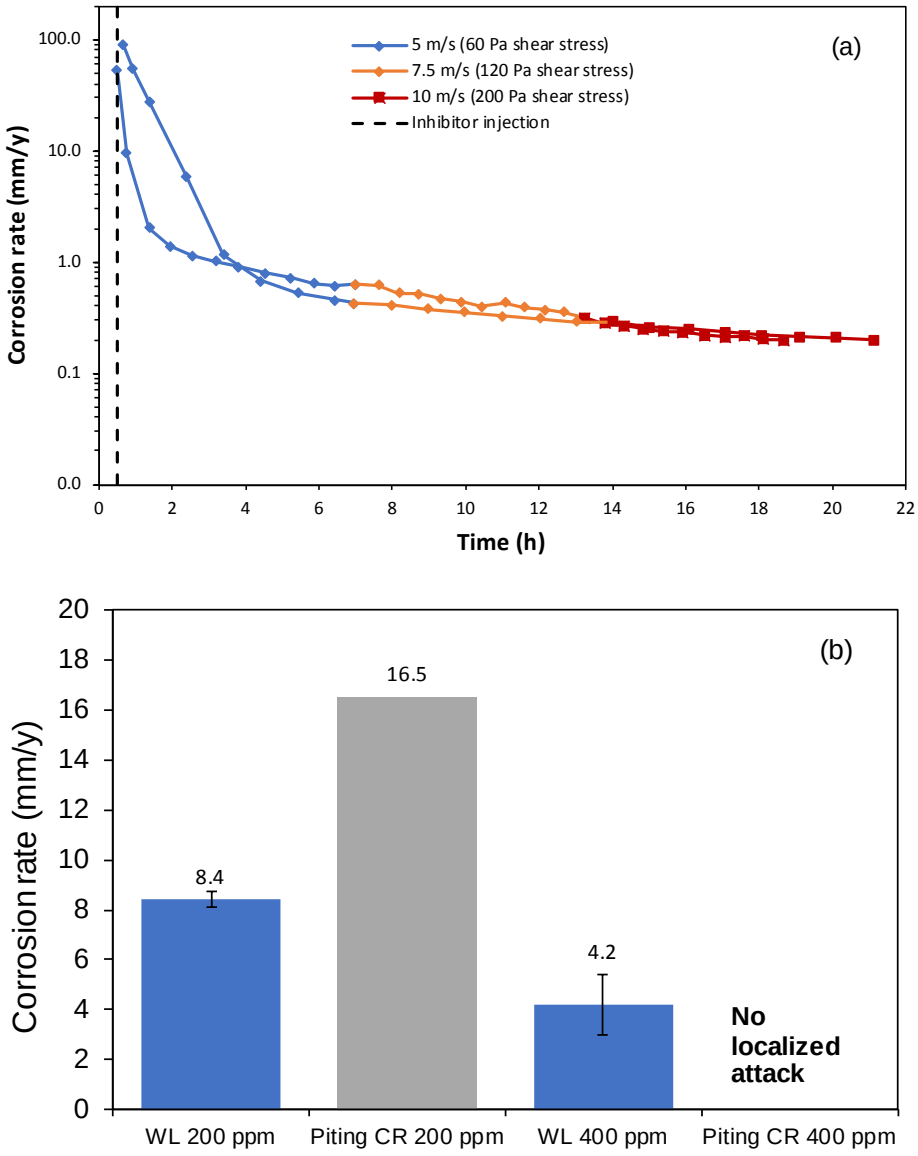

Figure 12: (a) LPR corrosion rate (b) WL and pitting corrosion rate comparisons for inhibitor "B" at concentrations of 200 ppm and 400 ppm. (90ºC, *p*CO2 = 3.3 bar, HAc = 500 ppm).

Effect of HAc on pit propagation

It has been reported by Amri et.al.[15] that the presence of HAc could increase the pit propagation of carbon steel exposed to CO_2 corrosion. Their studies were performed by means of an artificial pit. To study the effect of HAc on pit propagation inhibitor "A" was selected since this inhibitor promoted the occurrence of localized corrosion. Figure 13(a) shows the LPR corrosion rate with and without HAc. The corrosion rate without HAc and before injecting the corrosion inhibitor was 53.8 mm/y, while with 500 ppm of HAc was 92.6 mm/y. After adding the corrosion inhibitor the corrosion rate decreased sharply, reaching similar corrosion rates. In both cases the corrosion rate was time dependent. A comparison between the WL and pitting corrosion rates is shown in Figure 13(b). The WL corrosion rate was 2.5 bigger in the presence of HAc. The effect of HAc on pit propagation is clearly observed by a 4.5 times increase on the pit penetrations rate. The question remains if pits would keep propagating in a longer test. Amri et.al.[15] suggested a depletion of HAc inside the pit and alkalization that could favor the formation of iron carbonate ($FeCO_3$) and therefore stopping of the pit growth.

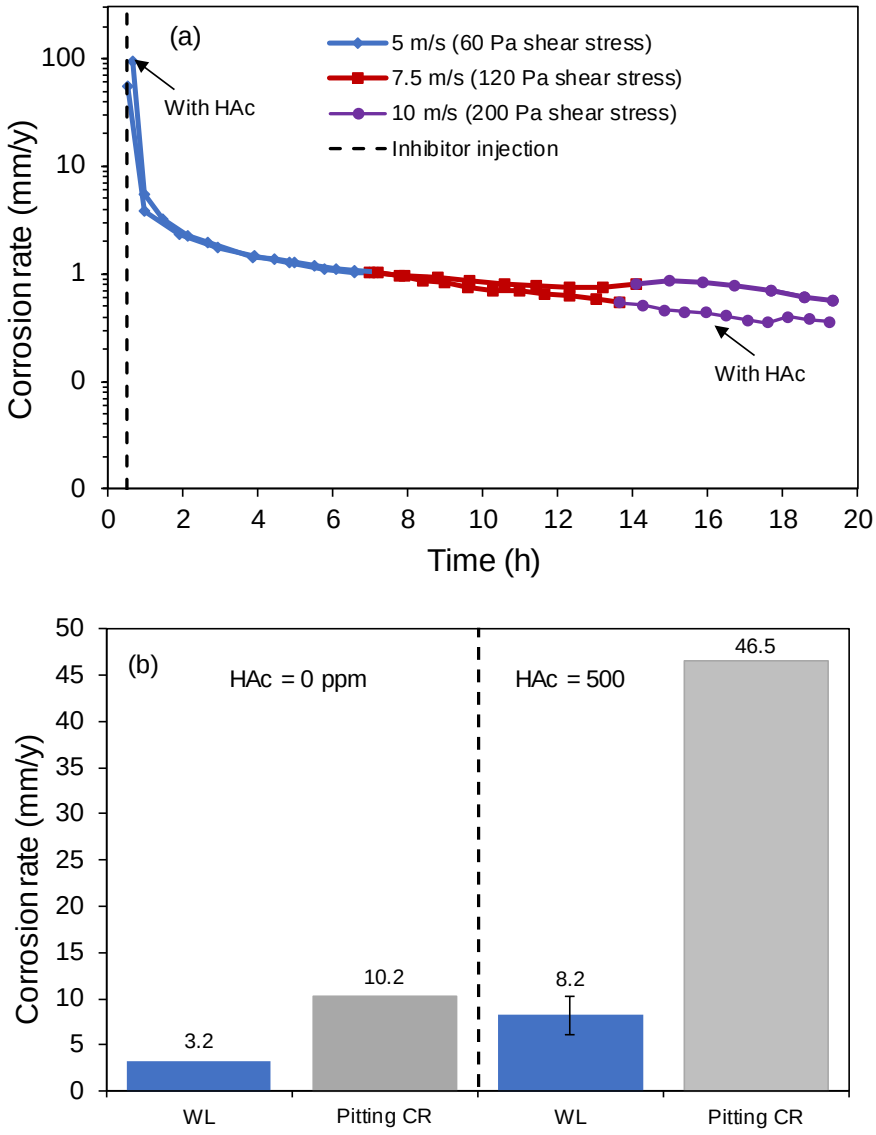

Figure 13: (a) LPR corrosion rate (b) WL and pitting corrosion rate comparisons for inhibitor "A" with and without HAc. (90°C, *p*CO2 = 3.3 bar).

CONCLUSIONS

The impact of high flow rates, acetic acid and inhibitor concentration on the performance of five corrosion inhibitors use to mitigate CO_2 corrosion of carbon steels was evaluated by linear polarization resistance, weight loss method and profilometry analysis. High inhibition efficiencies to mitigate general corrosion were observed for all the tested inhibitors. However, it was demonstrated that electrochemical measurements and weight loss method are not enough to determine if a corrosion inhibitor is effective. Analysis of the steel surface is crucial to determine the likelihood of localized attack especially at high flow rates where the injection of the wrong inhibitor concentration could lead to localized corrosion.

ACKNOWLEDGEMENTS

The principal author of this manuscript would like to thank Dr. Young from the Institute for Corrosion and Multiphase Technology at Ohio University, for his discussions while developing this project.

REFERENCES

1. Hausler RH, Schmitt G. “Hydrodynamic and Flow Effects on Corrosion Inhibition.” In: *Corrosion/2004, Paper No. 04402 (Houston, TX: NACE, 2004)*.
2. Hobbs J. *“Reliable Corrosion Inhibition in the Oil and Gas Industry RR1023”*; 2014.
3. De Marco R, Durnie W, Jefferson A, Kinsella B, Crawford A. Persistence of Carbon Dioxide Corrosion Inhibitors. *Corrosion*. 2002;58(4):354-363.
4. Mora-Mendoza JL, Chacon-Nava JG, Zavala-Olivares G, González-Núnez MA, Turgoose S. Influence of turbulent flow on the localized corrosion process of mild steel with inhibited aqueous carbon dioxide systems. *Corrosion*. 2002;58(7):608-619.
5. Zeng L, Zhang GA, Guo XP. Effect of hydrodynamics on the inhibition effect of thioureido imidazoline inhibitor for the flow accelerated corrosion of X65 pipeline steel. *Corrosion*. 2016;72(5):598-614.
6. Xiong Y, Brown B, Kinsella B, Nešic S, Pailleret A. Atomic Force Microscopy Study of the Adsorption of Surfactant Corrosion Inhibitor Films. *Corrosion*. 2014;70(3):247-260.
7. Li W, Pots BFM, Zhong X, Nesic S. Inhibition of CO 2 corrosion of mild steel − Study of mechanical effects of highly turbulent disturbed flow. *Corros Sci*. 2017;126:208-226.
8. Stern M, Geary A. Electrochemical polarization I. A theoretical analysis of the shape of polarization curves. *J Electrochem Soc*. 1957;104:56.
9. Tran T, Brown B, Nesic S, Tribollet B. Investigation of the Mechanism for Acetic Acid Corrosion of Mild Steel. *Corrosion*. 2014;70(3):223-229.
10. Crolet JL, Thevenot N, Nesic S. Role of Conductive Corrosion Products in the Protectiveness of Corrosion Layers. *Corrosion*. 1998;54(3):194-203.
11. Okafor PC, Nesic S. Effect of Acetic Acid on CO2 Corrosion of Carbon Steel in Vapor-Water Two-Phase Horizontal Flow. *Chem Eng Commun*. 2007;194(2):141-157.
12. Berntsen T, Seiersten M, Hemmingsen T. Effect of FeCO3 supersaturation and carbide exposure on the CO2 corrosion rate of carbon steel. *Corrosion*. 2013;69(6):601-613.
13. Jovancicevic V, Ramachandran S, Prince P. Inhibition of Carbon Dioxide Corrosion of Mild Steel by Imidazolines and Their Precursors. *Corrosion*. 1999;55(5):449-455.
14. Gusmano G, Labella P, Montesperelli G, Privitera A, Tassinari S. Study of the Inhibition Mechanism of Imidazolines by Electrochemical Impedance Spectroscopy. *Corrosion*. 2006;62(7):576-583.
15. Amri J, Gulbrandsen E, Nogueira RP. The effect of acetic acid on the pit propagation in CO2 corrosion of carbon steel. *Electrochem commun*. 2008;10(2):200-203.